Analysis of Thermal Conditions of the 6-m BTA Telescope Elements and the Telescope Dome Space

E. V. Emelianov
Special Astrophysical Observatory

The results obtained using the temperature monitoring systems of the 6-m BTA telescope primary mirror, dome space, and external environment are reported. We consider the factors that affect the development of microturbulence in the near-mirror air layer and inside the dome space, variation of the telescope focal length with the temperature of its structures, variation of seeing due to temperature gradients inside the primary mirror of the 6-m telescope. The methods used in various observatories for reducing microturbulence are analyzed. We formulate suggestions concerning the improvement of the temperature monitoring system currently in operation and the system of automatic adjustment of the telescope focal length to compensate the thermal drift of the focus during observations.

1. INTRODUCTION

1.1. *Effect of Telescope Mirror Thermal Condition on Degradation of Astronomical Seeing*

The most commonly used method for the analysis of seeing involve the use of a differential image motion monitor (DIMM). Such observations were performed in 1993 at Siding Spring Observatory [1]. The results were compared with the seeing achieved at the focus of the 3.9-m Anglo-Australian telescope (AAT). In addition to the estimates mentioned above, this analysis used the temperatures of the primary mirror, dome space, and external environment.

The above authors found seeing to be strictly anticorrelated with the temperature difference between the mirror and the dome space in the case where the mirror temperature was higher than the external air temperature: seeing deteriorated by $1''$ compared to DIMM readings with each degree of temperature difference. No seeing deterioration was observed in the cases where the mirror was cooler than the dome space air.

A compact cooling facility has been developed to improve seeing in observations with the 8.3-m Subaru telescope (Japanese instrument installed on Maua-Kea in Hawaii): the telescope mirror was blown with cool air right inside the mount [2]. Such a location of the cooling system allowed bringing the mirror to the operating condition much more efficiently.

Correlating the night temperatures based on weather forecasts for Mauna-Kea with the actual night temperatures the above authors pointed out that the difference did not exceed $\pm 2^\circ$C in 80% of the cases. Thus, given a weather forecast, it became possible to bring the mirror to temperatures that would be certainly lower than the night temperature well in advance (in daytime). To prevent the formation of condensate on the mirror and inside the mount, a complex facility has been developed to control the temperature of the mirror and that of the cool air in the control system in order to avoid the dew point. This facility was also partially used during observations: the compressor evacuating hot air from under the mirror continued to operate. As a result, the air heated by the actuators of the active mirror was evacuated from the mount, thereby reducing the heating of the Subaru mirror by the telescope mechanics.

Measurements showed that even such preobservational preparation of the mirror improves seeing by at least $0.1''$. Given the slower response of the primary mirror of the 6-m telescope, introducing a similar facility for it would bring even better results. However, in this case problems arise with ensuring fast uniform cooling of the entire volume of the primary mirror of the 6-m telescope and with the accuracy of weather forecasts.

Experiments with a heated spherical mirror showed that laminar air flow with a velocity of about $1\,\mathrm{ms}^{-1}$ can "blow off" microturbulent currents arising in the near-surface air layer. Without active air blow, microturbulent currents in the near-mirror layer degrade seeing at $Z < 45^\circ$ [3].

Seeing degradation is most pronounced at small mirror inclinations, i.e., for objects with $Z \lesssim 10^\circ$. For these areas seeing degradation is a factor of three to five stronger than in the cases where the mirror is tilted by 50°. However, laminar airflow blowing over the mirror surface at a speed of $1\,\mathrm{ms}^{-1}$ improves seeing significantly at small Z (at large Z this airflow has the opposite effect degrading the seeing).

The best way to "blow off" microturbulent currents in the near-surface layer of large mirrors would be to place the air blower horn in the central hole of the mirror for the air flow to spread off the center.

An automatic system for producing the air flow to blow the surface of the mirror of the 6-m telescope would make it possible to significantly improve the seeing for observations at $Z \lesssim 10^\circ$ even in the cases where the mirror temperature exceeds significantly the ambient air temperature (by $5 \div 10^\circ$C). By analogy with the 2.5-m INT telescope (during its op-

eration in the Greenwich Observatory), one can say that such measures would reduce the seeing FWHM in the cases of maximum temperature differences for the 6-m telescope (when the mirror temperature exceeds the ambient air temperature by 10°C) down to about one and a half widths of the turbulent atmospheric disk.

In order to develop active optics, a prototype telescope has been made at the National Astronomical Observatory of Japan with a monolithic 61-cm diameter 2.1-cm thick primary pyrex mirror [4]. The shape of the mirror was controlled by 12 actuators. A Shack–Hartmann sensor was used to analyze the wavefront. This experiment had a byproduct consisting in the analysis of seeing variations caused by turbulence in the near-mirror air layer, arising when the temperature of the mirror was higher than the air temperature inside the dome.

Wavefront distortions can be analytically characterized by the Zernike coefficients. As a combined seeing characteristic, we can use the Strehl ratio:

$$S = 1 - 2\pi^2 \mathrm{STR}^2/\lambda^2,$$

where STR^2 is the weighted sum of squared Zernike coefficients over the radial order. The closer is S to unity, the better will be the seeing.

Experiments performed by the above authors also showed seeing to degrade with increasing temperature of the primary mirror because of turbulent air currents arising in the near-mirror layer. To ensure seeing $S > 0.8$, the mirror temperature should be maintained at a level no higher than 1°C above the ambient air temperature inside the dome.

To reduce the effect of microturbulence in the near-mirror layer, the above authors proposed to "blow off" microturbulent currents by laminar air flow. To this end, an air blower with a wide horn was installed near the edge of the mirror. The laminar air flow blowing above the mirror surface at a speed of $1\,\mathrm{ms}^{-1}$ (results identical to those obtained by [3]) can reduce the seeing degradation by a factor of two (in terms of the Strehl ratio). For seeing degradation to become measurable, it is sufficient to heat the mirror by 0.2°C above the ambient air temperature.

Turbulence is usually characterized by the Rayleigh number. However, in our case a component of the Rayleigh number, the Brunt–Väisälä frequency [4], can be used as an objective characteristic of turbulence:

$$N = \sqrt{-\frac{G}{\rho(0)}\frac{\partial\rho(h)}{\partial h}},$$

where G is the gravitational constant, and $\rho(h)$ is the vertical density profile of gas.

Convective instability sets in if $N^2 < 0$. We now obtain, passing from density to air temperature:

$$N^2 = (G/c_p - \frac{\partial T}{\partial h})G/T,$$

where c_p is the specific heat capacity at constant pressure, and T is the absolute air temperature. Thus, reconstructing an accurate vertical theoretical temperature profile in the air column would allow is to determine whether air in it is convectively stable or form turbulent currents.

The root mean squared velocity of turbulent currents can be computed from known air temperature gradients:

$$v^2 = (\mathrm{grad}\, T_h - g/c_p)Lg/\sqrt{2}T,$$

where L is the mixing length (about 5–20 cm).

However, serious technical challenges should be addressed to measure the parameters of microturbulence arising inside the dome and in the near-mirror air layer by analyzing temperature gradients: one has not only fill the dome space with many temperature sensors, placing them apart from each other no farther than the mixing length, but also very accurately calibrate these sensors and take readings frequently enough with an accuracy of several hundredths of a degree!

1.2. Effect of Thermal Condition Inside the Dome on Degradation of Astronomical Seeing

Models of microturbulent air motions inside the dome are special cases of the Kolmogorov model for closed finite volumes. The most popular among them are the von Karman, Greenwood–Tarazano, and exponential models [5].

The refinement of a particular turbulence model is necessary for computing the characteristic size of turbulent regions and the coherence time. One of the possible options for the microturbulence detector is a device whose principle of operation is similar to that of the DIMM. In its base configuration, the device has the form of a fiber laser beam splitter to produce several coherent rays, which are transformed by a collimator into about 2-cm diameter parallel light beams (2 cm is the minimum size of a microturbulent region). The beams pass the region studied at different distances from each other and are then directed by a system of diagonal mirrors to the focus of a small telescope. Such a device can be used to study the characteristic spatial and temporal frequencies of microturbulence.

Turbulent air flow can be generally characterized by the standard deviation of the velocity of air currents, σ_v, or the fractional fluctuation of velocity,

$I = \sigma_v/\overline{v}$, where $\overline{v}$ is the average velocity of air currents [6].

Empirical measurements of the turbulent current properties inside the dome can be performed with a sensitive mechanical or ultrasound anemometer.

1.3. Effect of Thermal Condition of the Primary Mirror and Its Metal Structures on the Position of the Focal Plane

In the case of long-exposure photometric and spectroscopic observations (this especially concerns photometry), it is very important not only to maintain the image at the same position but also to maintain the constant focal distance. The focal distance of a telescope varies because of thermal deformations of its supporting structures and optical surfaces.

Variations of the focal length of the telescope resulting from thermal deformations of the mirror and supporting structures usually have the same sign (if only the operating surface of the mirror is open and all other sides are thermally insulated), and therefore in the case of sufficiently slow temperature variations the focal plane remains fixed relative to the flange of the primary focus.

If the mirror is not sufficiently thermally insulated, then thermal variations of the focus due to mirror bending and variation of the length of the telescope rods would have different signs: in the case of heating the curvature radius of the mirror decreases, whereas the rod length increases [7].

Although thermal deformations of the mirror show up much slowly than the rod deformations, they also contribute to the overall focus shift. Hence in the simplest linear model (if we neglect many other factors causing the shift of the telescope focus) the focal length of the telescope depends on the temperature of the primary mirror and the rod temperature as:

$$F = F_0 + (T_M - T_0) \cdot f_M + (T_B - T_0) \cdot f_B,$$

where F_0 is focus position at temperature T_0; T_M is the temperature of the mirror; T_B is the temperature of the rods of the telescope "tube" structure; f_M is the linear contribution of mirror deformations to the variation of the focus; f_B is the linear contribution of the deformation of the supporting structures of the telescope to the variation of the focus.

We thus see that even deriving the most elementary linear approximation to describe the temperature dependence of the focus position requires constructing a two-dimensional experimental function: the dependence of the focus on the mirror temperature and the temperature of the metal structures. Because of the large mass of the 6-m telescope primary mirror, thermal distortion of its shape is a slow process, i.e., thermal variation of the position of the focus during the night would be determined by the temperature of metal structures exclusively.

However, even such a simple approximation is inexact: the deformation of the mirror depends more on the temperature gradient field inside the mirror rather than on the temperature proper. We are thus dealing with a three-dimensional function even if we ignore less significant factors affecting the position of the focus.

The results of theoretical calculations lead us to conclude that reconstruction of the exact dependence of the telescope focal length on the temperatures of its constituent structures is a rather complicated task. However, we can try to reconstruct with some accuracy a particular dependence: the temperature dependence of the focal length during a certain observing night. The temperature of the mirror cannot change significantly overnight, and therefore focus variation is determined mostly by the contribution of the metal structures of the telescope. The error in this case is determined by many external factors (including the variation of seeing during the night), and therefore we cannot guarantee high accuracy even in terms of this approximation (we even cannot guarantee that automatic correction of the position of the focal plane would be sufficiently accurate to within ± 0.1 mm).

2. TEMPERATURE MONITORING SYSTEM FOR THE UNITS OF THE 6-M TELESCOPE AND THE AIR INSIDE THE DOME

According to the documentation [8], at the butt end of the primary mirror of the 6-m telescope a total of sixty 310-mm diameter 430-mm deep blind holes have been made to accommodate the mirror support unit (57 unloading and 3 defining support mechanisms). Also the mirror has six about 10-mm deep areas for jacking pads and one through hole with a diameter of 350/360 mm for the centering shell.

The mirror is a 655 ± 0.3 mm thick 6050 ± 5 mm diameter meniscus with surface radii of 48050 ± 50 mm. Each support mechanism shares 1/60 part of the mirror weight (i.e., about 700 kg). The upper part of the support is separated from the mirror by an air gap, where a temperature sensor can be placed.

In December 2008 the technical specification for the development of a multichannel data acquisition system to measure and store the temperatures of the 6-m telescope units, dome, and interpanel space has been approved. V. M. Kravchenko was in charge of installing temperature sensors, and S. I. Sinyavskii dealt with connecting them to the data acquisition system.

Temperature measurements are made with uncalibrated TS-1288 temperature sensors with an accu-

racy of 0.5°C or better. The M-FK-422 detectors were used to measure the temperatures of the telescope structures and dome panels (the temperature measurement error does not exceed 0.5°C). The detectors were not calibrated, and therefore their readings may differ by more than 0.5°C.

Installation of sensors was completed by June 2010, however only part of them have been connected to the data acquisition system. The sensors are connected to networked TRM-138 eight-channel gauge devices. Some of the sensors measure the air temperature, and some of them — the temperature of metal structures and side surfaces of the 6-m telescope primary mirror.

The data archiving system and the web interface [9] for working with the archive were developed by S. V. Karpov. The readings from all temperature sensors connected to the system are written to a PostgreSQL database at 15-min intervals. The web interface or the local service allow the required data to be extracted for any time interval when the system was operational.

Sensors for measuring the temperature of the primary mirror are arranged nonuniformly, and therefore to measure the temperature gradients inside the mirror, these sensors should be not only calibrated but also rearranged more uniformly. Placing temperature sensors in the hollows for support mechanisms would make it possible to monitor temperature gradients inside the mirror body. The linear thermal expansion coefficient, α_L, of the S-316 glass used to make the blank of the primary mirror of the 6-m telescope is equal to $(3.0 \div 3.1) \cdot 10^{-6}\,^{\circ}\mathrm{C}^{-1}$. For $\alpha_L = 3 \cdot 10^{-6}\,^{\circ}\mathrm{C}^{-1}$ a one-wavelength ($\lambda = 500\,\mathrm{nm}$) large warping of the shape of the mirror between two chosen points would be observed in the case of the 0.25°C temperature difference (if the temperature gradient is strictly radial). Thus, temperature registration for the 6-m telescope primary mirror should be accurate to within at least ±0.1°C.

A proper choice of the type of temperature sensors for measuring the distribution of temperature gradients in the 6-m telescope primary mirror would allow the calibrating temperature interval to be reduced based on the accumulated statistics of mirror temperatures. For instance, the temperature of the mirror remained within the −7°C to +21°C interval throughout the three-year interval from December 23, 2010 through January 23, 2014. Such a reduction of the temperature interval makes it possible to significantly improve the measurement accuracy.

In the temperature interval mentioned above, digital TSic 506 temperature sensors with the ZACwire interface can be used. The operating temperature measurement interval of these sensors spans from −10°C to +60°C. The rated accuracy throughout the entire operating range is ±0.3°C or better (with a discretization of about ±0.03°C). According to the rating data, a twofold reduction of the width of the measured temperature range allows the relative accuracy of measurements to be significantly improved. Calibrating the sensors for the temperature interval mentioned above reduced the measurement error down to ±0.1°C.

Another type of temperature sensors, TSYS 01 (with the SPI and I^2C interfaces), have a rated accuracy of $\pm(0.05 \div 0.1)$°C and the operating temperature range spanning fromт −40°C to +125°C. The use of such digital temperature sensors would simplify the temperature monitoring system and significantly improve its accuracy.

3. REDUCTION OF TEMPERATURE DATA

3.1. Thermodynamics of the Dome Space

The air volume in the dome space is equal to about $23000\,\mathrm{m}^3$. Its variation with temperature is due mostly to the following processes:

1. heating of the dome walls during daytime as a result of partial absorption of sunlight (insolation);
2. heat exchange with the ambient environment via dome walls (mostly as a result of heat transfer);
3. heat transfer as a result of the contact of air with the floor and lower part of the walls of the dome space;
4. penetration of warm air currents from the lower levels of the tower into the airspace of the dome room (oil exchange, space heating, and other systems).

To protect the dome space of the 6-m telescope against heating due to insolation, the dome has been made with double-layered walls and ventilated gap between the walls. In addition, such a double-layered structure of the dome walls reduces the efficiency of heat exchange with the ambient environment.

According to the report by L. I. Snezhko [10], the qualification of the thermal protection system of the 6-m telescope performed in 1994 showed that:

- the dome efficiently protects the telescope against insolation (i.e., the effect of the factor mentioned in item no. 1 above has been reduced practically to zero);
- temperature inside the dome is distributed uniformly (to within the sensitivity of the method of detection employed), only heating by 0.2°C of the prime focus cell by observational equipment is detected;

- the main source of heat release, the oil feed system, stands out by the high temperature of oleoducts and elevated (by about $\sim 1^\circ$C) temperature of the slewing ring and exit points of warm air from the hydrostatic bearing room.

In 2002 extensive work has been carried out in order to upgrade the oil feed system of the engines of the 6-m telescope (Yu. M. Mametiev, A. M. Pritychenko) [11]. The upgrade reduced substantially the power consumption and allowed cooling the oil before feeding it to the drives. As a result, the heat output to the dome space of the 6-m telescope has been reduced.

To cool the air in the dome space to maintain the temperature of the primary mirror of the 6-m telescope in the working range, the conditioning system has been overhauled (PishcheAgroStroyProekt, OAO). Three 30-kW freon compressor units were installed in the technical unit located outside the tower of the 6-m telescope. These compressor units are used to cool the coolant consisting of 35% ethylene glycol solution, which is then pumped to air exchange devices installed in the dome and under-floor space. To thaw the ice that forms on air-exchange devices, electrical heaters with a total power of about 100 kW are used.

The icing intensity on cool conductors and air interchanges increases with increasing temperature difference between the dome space and coolant, resulting in increased energy consumption for defrosting and reduced efficiency of the upgraded cooling system [12].

The efficiency of this system can be demonstrated by simple thermodynamic computations.

3.1.1. Adiabatic Approximation

We first compute the time required for the cooling system to reduce the air temperature in the dome space by 10°C (to achieve the maximum permissible mirror cooling rate, 2°C per day [10]).

In the absence of heat exchange with the ambient environment air temperature varies isochorically (with a slight change of pressure due to the change of temperature), then isobarically (due to the air exchange with the ambient environment). Strictly speaking, isobaric variation of temperature alone is sufficient to compromise the adiabatic approximation considered, and therefore we assume the process to be isochoric to a first approximation.

Let us now compute the amount of heat to be withdrawn from the dome space air to cool it by dT°C (hereafter we adopt the main computational formulas from [13, 14]):

$$c_V = \frac{i}{2}\frac{R}{M}, \qquad dQ = mc_V\,dT = \rho V\frac{i}{2}\frac{R}{M}\,dT$$

$$dQ = 1.29 \cdot 23000 \cdot \frac{5}{2}\frac{8.31}{29 \cdot 10^{-3}}\,dT = 2.13 \cdot 10^7\,dT \text{ [J]},$$

where c_V is the constant volume specific heat; i is the number of degrees of freedom of ideal-gas particles; M, the molar mass of the air; R, the universal gas constant; ρ, the air density; Q, the amount of heat, and T, the temperature.

Thus to cool the dome space air by 10°C, we have to withdraw from it about 213 MJ of energy.

The total cooling capacity of the cooling system is of about 107 kW. The minimum time required to withdraw 213 MJ of energy from the dome space air (without the time required for forced mixing of air) is in this case

$$t_{min} = \frac{2.13 \cdot 10^8}{1.07 \cdot 10^5} \approx 2000\,\text{s},$$

i.e., about 33 min.

3.1.2. Computation of Heat Inflow

The heat current intensity from the floor and walls of the dome space depends on temperature gradient:

$$\frac{\partial Q}{dt\,dS} = -\kappa\frac{\partial T}{\partial x},$$

which increases sharply in the case of intense mixing (here κ is the air heat-conduction coefficient). Thus the heat output for the given gradient $\theta = \operatorname{grad} T$ is

$$P = -24.1 \cdot 10^{-3} S\theta \text{ [W]},$$

where S is the area of the surface with the given gradient θ. For example, the heat output of the floor is

$$P = -13.7\theta \text{ [W]}.$$

The heat output of the dome walls can be computed in a similar way ($P \approx -60\theta$).

Such a small heat current allows us to neglect the heating of air inside the dome caused by heat transfer from the walls and the floor. Hence the main source of air heating inside the dome are heat currents from living quarters and technological buildings.

L. I. Snezhko approximately computed the heat currents, which proved to correspond to a temperature increase rate of $1.4^\circ\text{C}\,\text{h}^{-1}$ equivalent to a heat output of about 8.3 kW.

Approximate computations show that the available cooling system, if it were perfect, would be capable of maintaining the temperature inside the dome at a level corresponding to the temperature difference of up to 10°C between the primary mirror and dome space air. The cooling capacity required to maintain the air temperature inside the

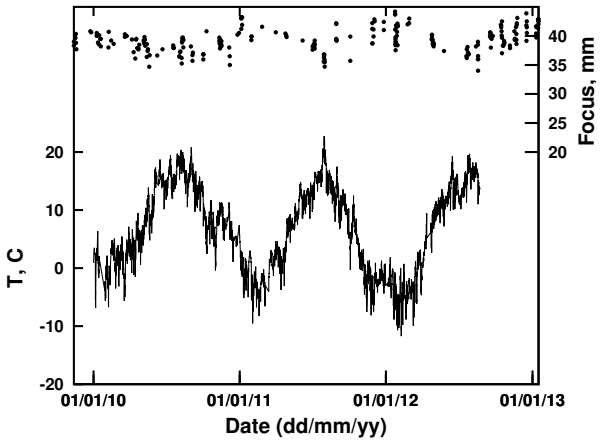

Figure 1. Rod temperature (the solid line) and focus readings (the dots) over three years.

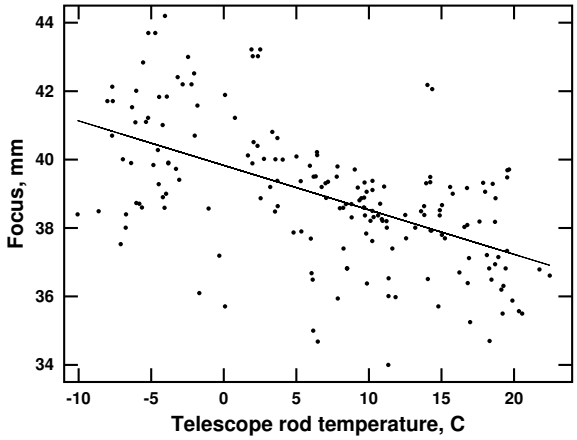

Figure 2. Relationship between focus measurements and rod temperature. The solid line shows a linear approximation.

dome at a given level can be estimated at 9–10 kW (L. I. Snezhko). However, given that the capacity of the air conditioning system inside the dome of the 6-m telescope depends heavily on the external air temperature and the difference between the external and internal temperatures, the efficiency of this system in wintertime would be low.

To achieve the maximum permissible cooling rate of the primary mirror, the air inside the dome should be gradually cooled until the mirror reaches the required temperature while maintaining constant temperature difference between the mirror and air in the process.

A detailed temperature monitoring of the dome space is needed to more accurately determine the temperature gradients and heat output of stray heat sources (and hence the amount of electric power needed to maintain the given temperature in the dome space).

3.2. Focus Position Temperature Dependence

To analyze the dependence of the position of the focus on the temperature of different telescope and dome parts, we selected the appropriate data for the past three years from the temperature archive and from ASPID database [15]. To this end, we

1. recursively scanned the directories with the archives to select from SCORPIO logs the strings following the text "focussing TELESCOPE" (i.e., information about images acquired after focussing the telescope);

2. generated archive names based on the names of retrieved files they contain;

3. unpacked all archives that we found to be of interest for us into the current directory;

4. copied the FITS header of the files whose names we obtained at step 1 into a separate file;

5. analyzed the `INSTRUME` and `IMAGETYP` fields of the FITS header to determine whether the given image was acquired on SCORPIO and whether the image type is "object"; if the condition was satisfied, we wrote into the log file the observing date and time, focus, and the temperatures of the mirror, domespace, and external environment.

We retrieved from the temperature archive the readings of the thermometer located on one of the telescope rods. We then averaged these data into 15-min bins (the database contains readings made at 10-s intervals). We performed all subsequent computations in Octave environment.

We adopted the focal lengths and temperatures from different archives based on measurements made with different sampling times (see Fig. 1), and therefore we had first to homogenize the observational data reducing them to a single system. To this end, we selected those focus measurements for which rod temperature measurements were available within 15 min from the focus-length measurement. We then interpolated the rod temperature to the image acquisition times on SCORPIO.

The correlation coefficient between the rod temperature and the measured focus lengths is equal to -0.56, and the linear interpolation of the relation (see Fig. 2) yields the following approximate formula

$$F \approx 39.83 - 0.13 \cdot T, \qquad \sigma_F = 1.64, \qquad (1)$$

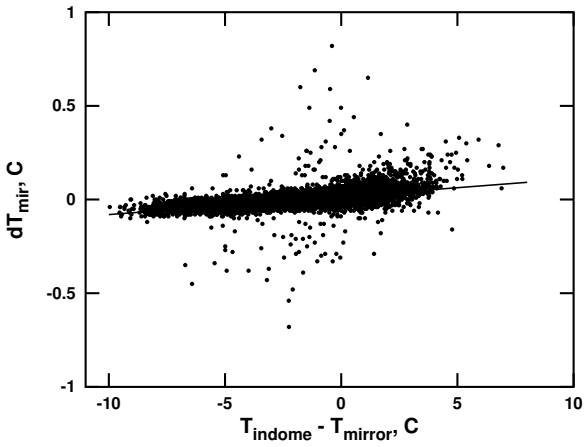

Figure 3. Relation between the rate of mirror temperature change and the temperature difference between the dome space and the mirror (data for the three-year period). The solid line shows a linear fit to the data.

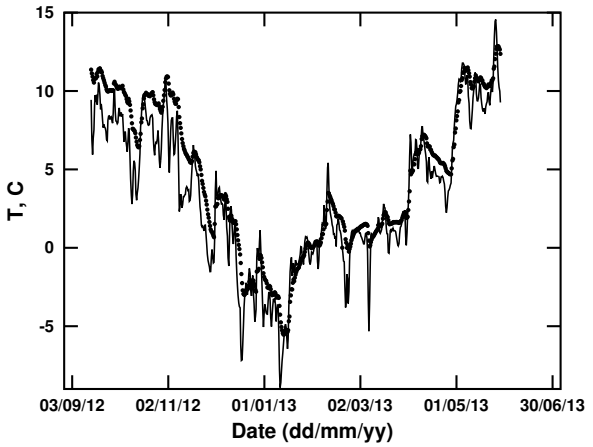

Figure 4. Temperature of the mirror (the dots) and one-day moving average of the dome-space temperature (the solid line) for a selected time interval.

where F are the focal length measurements in mm; T, the rod temperature in Celcius degrees, and σ_F, the standard deviation of the focal length.

An analysis of similar relationships between focus measurements and dome space and mirror temperatures yielded the following results. The correlation coefficient between the dome space temperature and focus measurements is equal to -0.54, and the corresponding linear approximation has the form $F \approx 39.53 - 0.13 \cdot T$, $\sigma_F = 1.67$, which is close to (1). The correlation coefficient for the mirror temperature was the highest among all (-0.66), and the corresponding linear approximation has the form $F \approx 40.22 - 0.17 \cdot T$, $\sigma_F = 1.49$. It is clear that in the latter case the resulting relation is more well defined, because the mirror acts as sort of temperature damper, which smooths rapid variations affecting the general correlation.

A detailed analysis of individual nights did not improve the statistics: the scatter of the data about linear approximation still remained too large to conclude about bona fide unique dependence of focus measurements on the readings of any temperature sensor.

The large data scatter in our case is due not solely to various errors, but also to the more complex form of the temperature dependence of the telescope focal length. Thus, e.g., in the case the detector is held by a sole steel rod and there are no other factors involved, the coefficient in dependence (1) would be equal to -0.31. Temperature gradients arising inside the mirror body in response to a change of its temperature would give rise to another, positive coefficient, and a well-defined dependence on the rate of change of the dome space temperature (because the variation of the temperature of the primary mirror of the 6-m telescope also depends on on it).

We can thus conclude that unambiguous automatic adjustment of the focal length in the process of observations without the need to readjust the focus by observing stars can be best achieved by installing a laser range finder on the prime focus cell and monitoring the distance from the prime focus cell to the spider support of the diagonal mirror or some point on the mirror mount. However, a careful calibration of temperature sensors and their rearrangement will make it possible to derive a unique analytical dependence.

3.3. Dependence of the Rate of Primary Mirror Temperature Change on the in-Dome Temperature

To construct this dependence, we retrieved from the archives the data concerning the temperature inside the dome and the temperature of the mirror averaged in one-hour bins. After differentiating the mirror temperature, $dT_{\rm mir}$, and computing the temperature difference ΔT between the dome space and the mirror, the resulting datasets were cleaned to remove analog-to-digital converter errors and surges due to the nonuniform distribution of measurements by rejecting the measurements with $|\Delta T| > 10^\circ$C and $|dT_{\rm mir}| > 1^\circ$C.

The correlation coefficient between $dT_{\rm mir}$ and ΔT is 0.52. Linear fit to all the data obtained (see Fig. 3) has the form:

$$dT_{\rm mir} \approx 0.0152 + 0.0096 \cdot \Delta T.$$

To perform the correlation analysis, we selected from the resulting data set ten time intervals with uniformly distributed temperature measurements.

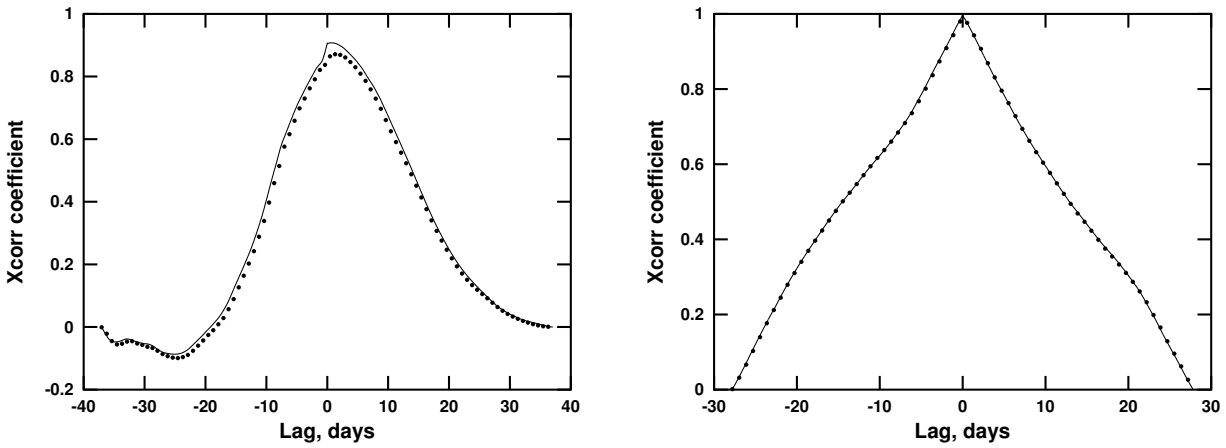

Figure 5. Cross-correlation function of the temperature of the 6-m telescope primary mirror and that of the dome space. The dots and solid lines show the temperatures averaged in one-hour and one-day bins respectively.

The longest continuous interval (see Fig. 4) spanned about 255 days (from September 14, 2012 through April 28, 2013). For each interval we constructedthe cross-correlation functions between the temperatures of the mirror and dome space, and derived linear approximations between the rate o change of the mirror temperature and that of the temperature difference between the dome space and the mirror.

The position of the maximum of the cross-correlation function for all selected time intervals varied from 41 hours (31 hours for the moving average) for January 2011 to zero for the other our intervals. The largest shift evidently is obtained for the case of time intervals with sharp changes of the temperature of the dome space. Zero shift corresponds to time intervals with smoothly varying daily averaged temperature, and also time intervals when the air conditioning system was switched on in the dome. For example, Fig. 5 shows the mutual correlation functions of the mirror and dome space temperature for the cases of nonzero and zero shifts.

Fitting the rate of change of the temperature of the primary mirror of the 6-m telescope as a function of the temperature difference between the dome space and the mirror for all ten intervals yielded an average coefficient of $0.01\,\mathrm{h}^{-1}$, which agrees with known values: for the temperature of the primary mirror of the 6-m telescope to change by 0.1°C in one hour, the temperature in the dome space should differ from the mirror temperature by 10°C.

The data obtained fully agree with the results of the computations performed by L. I. Snezhko. To study the processes caused by temperature gradients inside the primary mirror of the 6-m telescope, we have to place accurately calibrated temperature sensors in the supporting holes.

4. CONCLUSIONS

To sum up, we conclude that: first, there is no need to install a large number of temperature sensors inside the dome; second, for unambiguous assessment of the extra degradation of seeing due to temperature gradients and microturbulent air motions, it is necessary to measure the temperature of telescope rods at several points and the distribution of temperature inside the primary mirror. It is very important to ensure that all sensors have zero scatter of readings (within the permissible error) in the temperature interval from −10°C to +25°C. This means that all sensors should be accurately calibrated in a thermostat using a certified precision reference thermometer. The sensor readings should be converted into real temperatures both inside the data acquisition system and in the archiving server when the new portion of temperature measurements is written to the database.

The use of digital temperature sensors would make it possible to simplify the temperature monitoring system and improve its accuracy. Another option for the upgrade consists in the use of the available system carefully calibrating and rearranging the temperature sensors.

5. ACKNOWLEDGMENTS

I am grateful to Prof. V. L. Afanasiev for suggesting the idea of analyzing the dependence of the 6-m telescope focus position on temperature conditions and for describing the ASPID database structure. I am also grateful to Prof. V. E. Panchuk for valuable comments concerning the text of the paper. Observations on the 6-

m telescope of the Special Astrophysical Observatory are held with financial support from the Ministry of Education and Science of the Russian Federation (contract No. 14.619.21.0004, project identifier RFMEFI61914X0004).

1. P. R. Wood, S. G. Ryan. Publ. Astron. Soc. Australia. **12**, 95 (1995).
2. A. Miyashita, R. Ogasawara, G. Macaraya, N. Itoh. Publications of the National Astronomical Observatory of Japan, **7**, 25 (2003).
3. C. M. Lowne. Mon. Not. of Royal Astron. Soc. **188**, 249 (1979).
4. M. Iye, T. Noguchi, Y. Torii et al. Publ. Astron. Soc. Pacific. **103**, 712 (1991).
5. A. Ziad, D.-A. Wassila, J. Borgnino, M. Sarazin. Society of Photo-Optical Instrumentation Engineers (SPIE) Conference Series. **8444**, 844431 (2012).
6. L. Zago, F. Rigaut. The Messenger. **55**, 22 (1989).
7. C. D. Perrine. // Publ. Astron. Soc. Pacific. **30**, 30 (1918).
8. http://www.sao.ru/hq/sekbta/Tex_doc/Book1_view.pdf
9. http://acs4.sao.ru/meteo/can_requestor.php
10. L. I. Snezhko. Bull. Spec. Astrophys. Obs. **45**, 39 (1993).
11. http://www.sao.ru/hq/sekbta/Maslo/
12. http://www.sao.ru/hq/sekbta/Xolod/xolod_2.htm
13. D. V. Sivukhin, *General course of physics. Thermodynamics and molecular physics* (Nauka, Moscow, 1975) [in Russian].
14. I. V. Saveliev, *General physics course, Vol. 1: Mechanics, oscillations and waves, molecular physics* (Nauka, Moscow, 1970) [in Russian].
15. http://alcor.sao.ru/db/aspid/